15-μm 128 × 128 GaAs/Al$_x$Ga$_{1-x}$As Quantum Well Infrared Photodetector Focal Plane Array Camera

Sarath D. Gunapala, Jin S. Park, Gabby Sarusi, True-Lon Lin, John K. Liu,
Paul D. Maker, Richard E. Muller, Craig A. Shott, and Ted Hoelter

Abstract— In this paper, we discuss the development of very sensitive, very long wavelength infrared GaAs/Al$_x$Ga$_{1-x}$As quantum well infrared photodetectors (QWIP's) based on bound-to-quasi-bound intersubband transition, fabrication of random reflectors for efficient light coupling, and the demonstration of a 15-μm cutoff 128 × 128 focal plane array imaging camera. Excellent imagery, with a noise equivalent differential temperature ($NE\Delta T$) of 30 mK has been achieved.

I. INTRODUCTION

THERE are several applications that require very long wavelength, large, uniform, reproducible, low cost, low $1/f$ noise, low power dissipation, and radiation hard infrared (IR) focal plane arrays (FPA's). For example, the absorption lines of many gas molecules, such as ozone, water, carbon monoxide, carbon dioxide, and nitrous oxide occur in the wavelength region from 3 to 18 μm. Thus, IR imaging systems that operate in the very long wavelength IR (VWIR) region (12–18 μm) are also required in many space applications such as monitoring the global atmospheric temperature profiles, relative humidity profiles, cloud characteristics, and the distribution of minor constituents in the atmosphere which are being planned for NASA's Earth Observing System [1]. In addition, 12–18-μm FPA's would be very useful in detecting cold objects such as ballistic missiles in midcourse (when hot rocket engine is not burning most of the emission peaks are in the 8–15-μm IR region) [2]. The GaAs based Quantum Well Infrared Photodetector (QWIP) [3]–[5] is a potential candidate for such space borne applications and it can meet all of the requirements mentioned above for this spectral region.

Fig. 1 shows the schematic conduction band diagram of a typical *bound-to-continuum* QWIP [6] which utilizes bound-to-continuum intersubband absorption. By carefully designing the quantum well structure, as well as the light coupling to the detector, it is possible to optimize the material to have an optical response in the desired spectral range and determine the spectral response shape [7]. In QWIP's, the dark current originates from three different mechanisms [8]. As shown in Fig. 1, the dark current arising from the first process is due to quantum mechanical tunneling from well to well through the Al$_x$Ga$_{1-x}$As barriers (sequential tunneling). This process is independent of temperature. Sequential tunneling dominates the dark current at very low temperatures ($<$30 K for 15-μm QWIP's). The second mechanism is thermally assisted tunneling which involves a thermal excitation and tunneling through the tip of the barrier into the continuum energy levels. This process governs the dark current at medium temperatures. The third mechanism is classical thermionic emission and it dominates the dark current at higher temperatures ($>$45 K for 15-μm QWIP's). Consequently, for QWIP's operating at higher temperatures the last mechanism is the major source of dark current [8]. Therefore, the VWIR FPA we have discussed here in detail consisted of *bound-to-quasi-bound* QWIP's [9]. The advantage of the bound-to-quasi-bound QWIP over the bound-to-continuum QWIP [9] is that in the case of bound-to-quasi-bound QWIP the energy barrier for thermionic emission is the same as it is for photoionization as shown in Fig. 2. In the case of a bound-to-continuum QWIP the energy barrier for the thermionic emission is 10–15 meV less than the photoionization energy. Thus, the dark current of bound-to-quasi-bound QWIP's is reduced by an order of magnitude (i.e., $I_d \propto e^{-(\Delta E/kT)} \approx e^{-2}$ for $T = 55$ K).

II. TEST STRUCTURE RESULTS

The device structure consists of 50 periods containing 65 Å wells of GaAs (doped $n = 2 \times 10^{17}$ cm^{-3}) and 600 Å barriers of Al$_{0.15}$Ga$_{0.85}$As (sandwiched between 0.5-μm GaAs top and bottom contact layers doped $n = 2 \times 10^{17}$ cm^{-3}) grown on a semi-insulating GaAs substrate by molecular beam epitaxy (MBE). Then a 1.1-μm thick GaAs cap layer on top of 300 Å Al$_{0.15}$Ga$_{0.85}$As stop-etch layer was grown *in situ* on top of the device structure to fabricate the light coupling optical cavity. The MBE grown QWIP structure was processed into 200-μm diameter mesa test structures (area $= 3.14 \times 10^{-4}$ cm^2) using wet chemical etching, and Au/Ge ohmic contacts were evaporated onto the top and bottom contact layers. The dark current–voltage curves of the QWIP was measured as a function of temperature from $T = 30–60$ K and the $T = 55$ K curve, as shown in Fig. 2. The asymmetry in the dark current is attributed to the Si dopant migration into the growth direction [10] and hence higher asymmetry in the band structure.
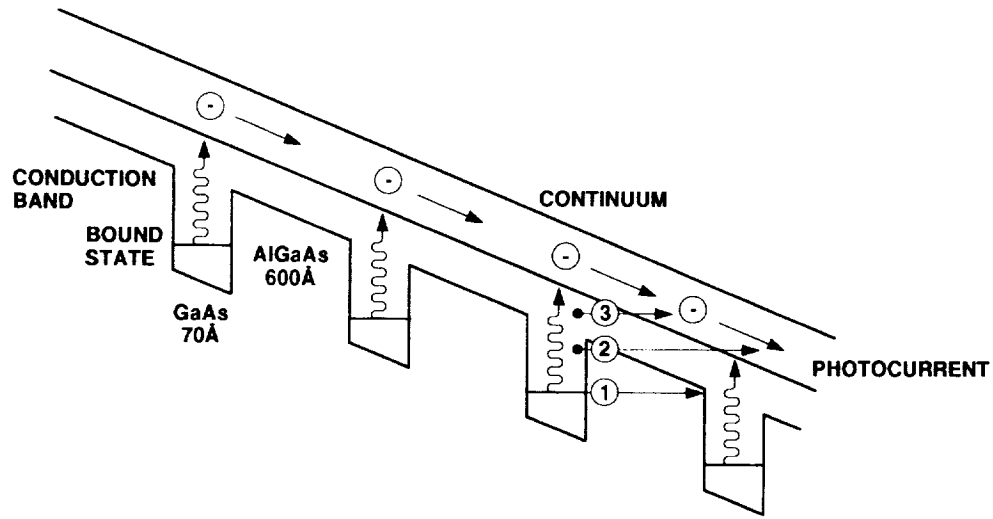
Fig. 1. Schematic diagram of the conduction band in a bound-to-continuum QWIP with an electric field. Absorption of IR photons can photoexcite electrons from the ground state of the quantum well into the continuum, causing a photocurrent. Three dark current mechanisms are also shown: 1) ground state tunneling; 2) thermally-assisted tunneling; and 3) thermionic emission.
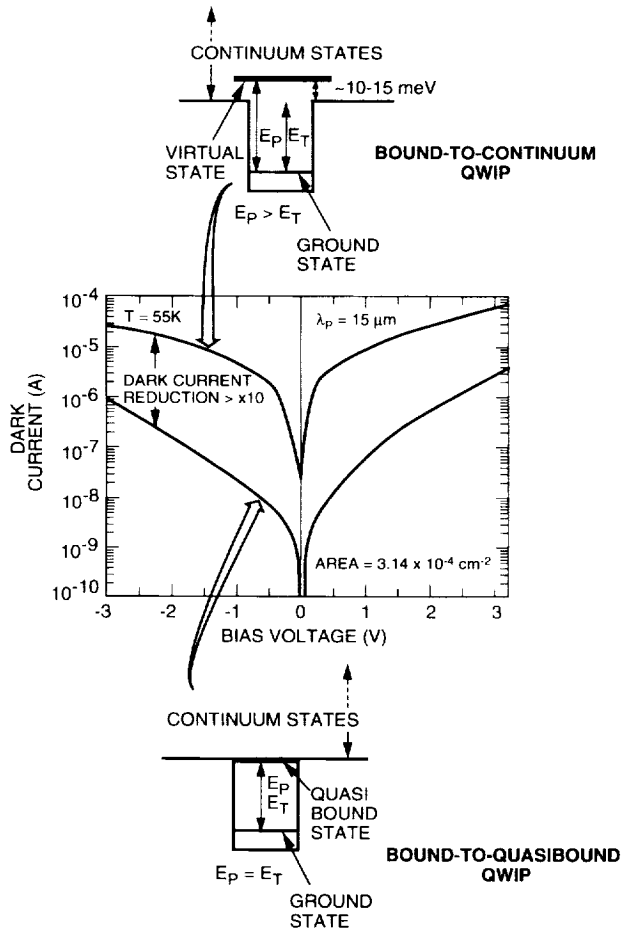

Fig. 2. Comparison of dark currents of bound-to-continuum and bound-to-quasi-continuum VWIR QWIP's as a function of bias voltage at temperature $T = 55$ K.
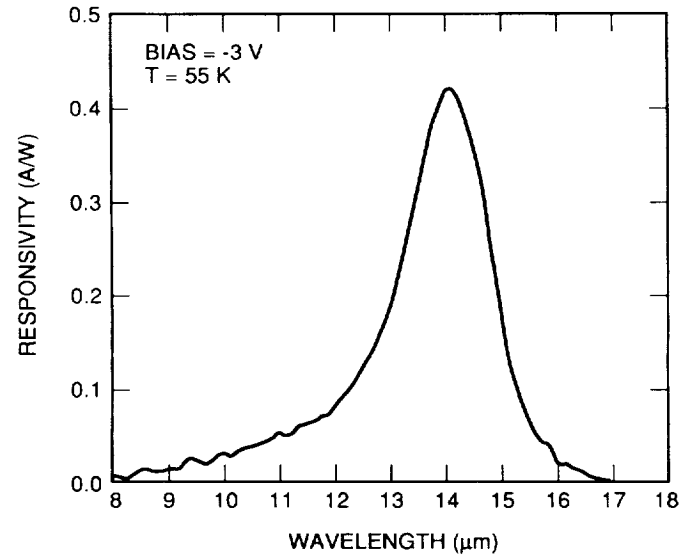

Fig. 3. Responsivity spectra of a bound-to-quasi-continuum VWIR QWIP focal plane array sample at temperature $T = 55$ K. The spectral response peak at 14.2 μm and the long wavelength cutoff is at 14.9 μm.

The responsivity spectra of these detectors were measured using a 1000 K blackbody source and a grating monochromator. The absolute peak responsivities (R_p) of the detectors were measured using a calibrated blackbody source. The

detector were back illuminated through a 45° polished facet [7] and its responsivity spectrum is shown in Fig. 3. The responsivity of the detector peak at 14.2 μm and the peak responsivity (R_p) of the detector is 420 mA/W. The spectral width and the cutoff wavelength are $\Delta\lambda/\lambda = 13\%$ and $\lambda_c = 14.9$ μm. The bias dependent peak responsivity of the detector is shown in Fig. 4. The measured absolute responsivity of the detector is small up to about $V_B = 1$ V. Beyond that it increases nearly linearly with the bias reaching $R_P = 560$ mA/W at $V_B = 4$ V. This type of behavior of responsivity versus bias is typical for a bound-to-quasi-bound QWIP. The peak quantum efficiency was 3% (lower quantum efficiency is due to the lower well doping density) for a 45° double pass.

The current noise i_n was measured using a spectrum analyzer and experimentally determined the photoconductive
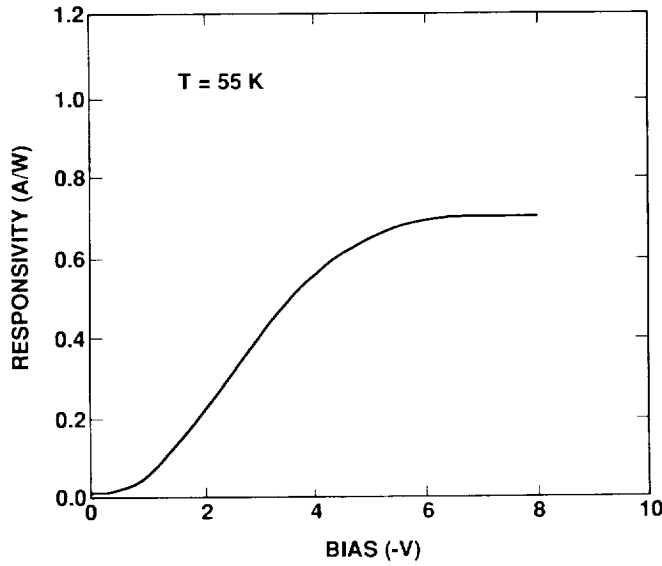
Fig. 4. Peak responsivity as a function of bias voltage at temperature $T = 55$ K.
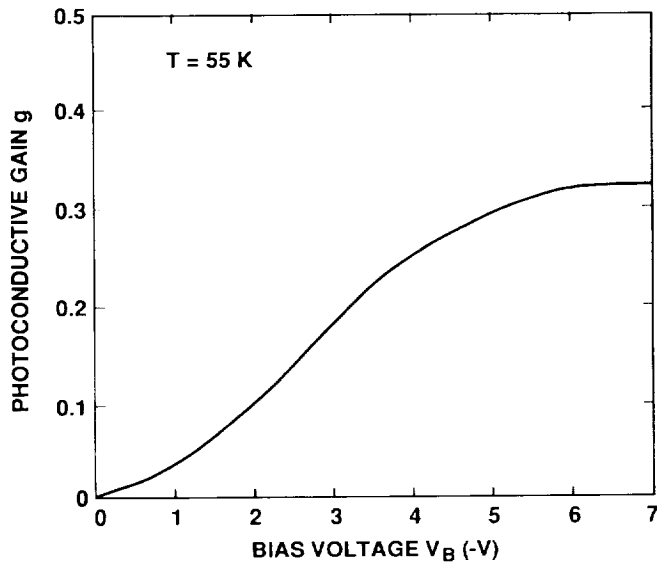

Fig. 5. Photoconductive gain as a function of bias voltage at temperature $T = 55K$.

Fig. 6. (a) Intersubband absorption process of QWIP's at normal incidence. (b) 45° polished facet light coupling.

gain [11] g using $g = i_n^2 \Delta f I_D B + 1/2N$. where B is the measurement bandwidth and N is the number of quantum wells. As shown in Fig. 5, photoconductive gain of the detector reached 0.32 at $V_B = -6$ V. Since the gain of QWIP is inversely proportional to the number of quantum wells N, the better comparison would be the well capture probability p_c, which is directly related to the gain [11] by $g = 1/Np_c$. The calculated well capture probabilities are 20% at low bias and 6% at high bias voltage which indicate the excellent hot-electron transport in this device structure. The peak detectivity is defined as $D_p^* = R_p \sqrt{A B}/i_n$, where R_p is the peak responsivity, A is the area of the detector and $A = 3.14 \times 10^{-4}$ cm². The measured peak detectivity at bias $V_B = -3$ V and temperature $T = 55$ K is 1.6×10^{10} cm/$\sqrt{\text{Hz}}$/W.
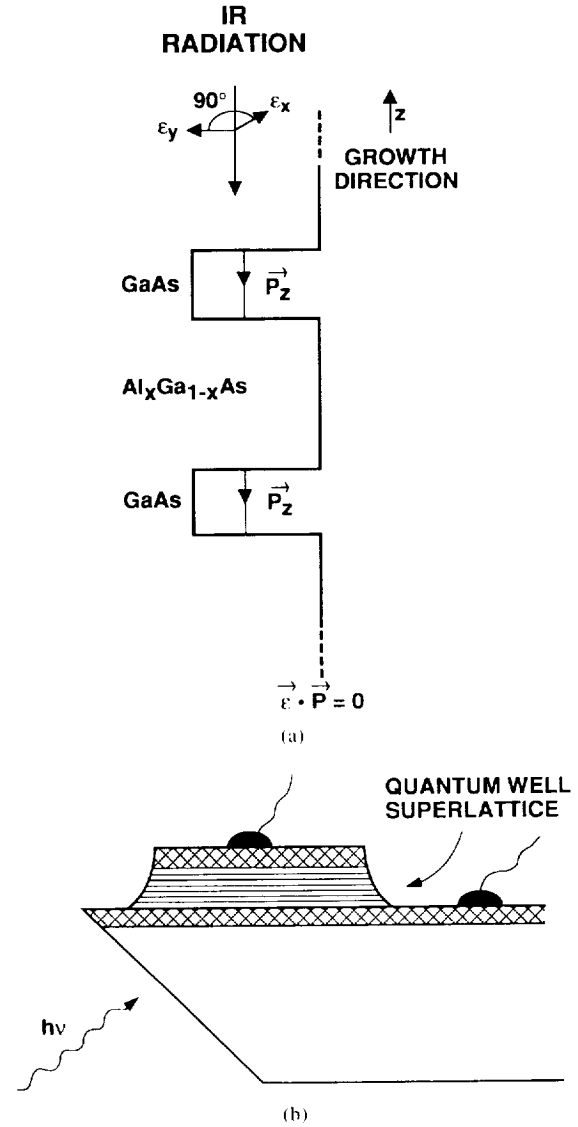
III. LIGHT COUPLING

QWIP's do not absorb radiation incident normal to the surface since the light polarization must have an electric field component normal to the superlattice (growth direction) to be absorbed by the confined carriers. As shown in Fig. 6(a) when the incoming light contains no polarization component along the growth direction, the matrix element of the interaction vanishes (i.e., $\vec{\varepsilon} \cdot \vec{p}_z = 0$ where $\vec{\varepsilon}$ is the polarization and $\vec{p}$ is the momentum along the z direction). As a consequence, these detectors have to be illuminated through a 45° polished facet [7] as shown in Fig. 6(b). Clearly, this illumination scheme limits the configuration of detectors to linear arrays and single elements. For imaging, it is necessary to be able to couple light uniformly to two-dimensional (2-D) arrays of these detectors.

Many more passes of IR light inside the detector structure can be obtained by incorporating a randomly roughened re-flecting surface on top of the detectors which also removes the light coupling limitations and makes 2-D QWIP imaging
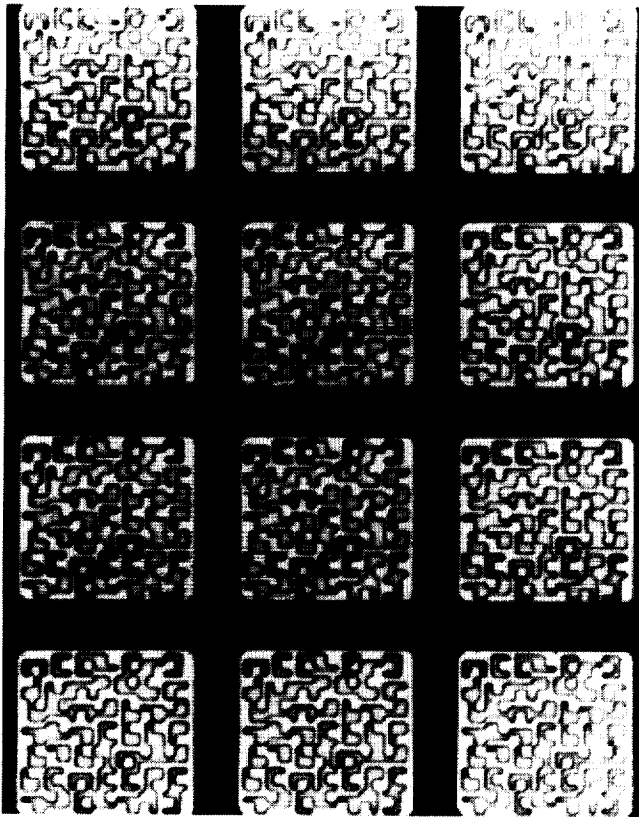
Fig. 8. Thirty-five 128 × 128 QWIP focal plane arrays on a 3-in GaAs wafer.

Fig. 7. Expanded corner of 128 × 128 QWIP FPA shows two level random reflectors on individual QWIP pixels (38 × 38 μm^2). The random reflectors increase the light coupling efficiency by a factor of eight when the substrate is thinned down to ~1 μm.

Fig. 9. Photosignal histogram of the 16384 pixel of the 128 × 128 array showing a high uniform uncorrected standard deviation of only $\sigma = 2.4\%$.

arrays feasible. A factor of eight enhancement in QWIP responsivity compared to 45° illumination geometry has been achieved with a randomly roughened reflecting surface [12]. The random structure on top of the detector prevents the light from being diffracted normally backward after the second bounce as happens in the case of cross-grating. After each bounce, light is scattered at a different random angle and the only chance for light to escape out of the detector is when it is reflected toward the surface within the critical angle of the normal. For the GaAs/air interface this angle is about 17°, defining a very narrow escape cone for the trapped light. The reflector was designed with two levels of scattering surfaces located at quarter wavelength separations, as shown in Fig. 7. The area of the top unetched level is equal to the area of the etched level ($\lambda/4$ deep). Therefore, the normally reflected light intensities from the top and bottom surfaces of random reflector are equal and 180° out of phase, thus maximizing the destructive interference at normal reflection and hence lowering the light leakage through the escape cone. This random structure was fabricated on the detectors by using standard photolithography and CCl_2F_2 selective dry etching. The advantage of the photolithographic process over a completely random process is the ability to accurately control the feature size and preserve the pixel to pixel uniformity which is a prerequisite for high sensitivity imaging focal plane arrays. Unlike periodic gratings the light
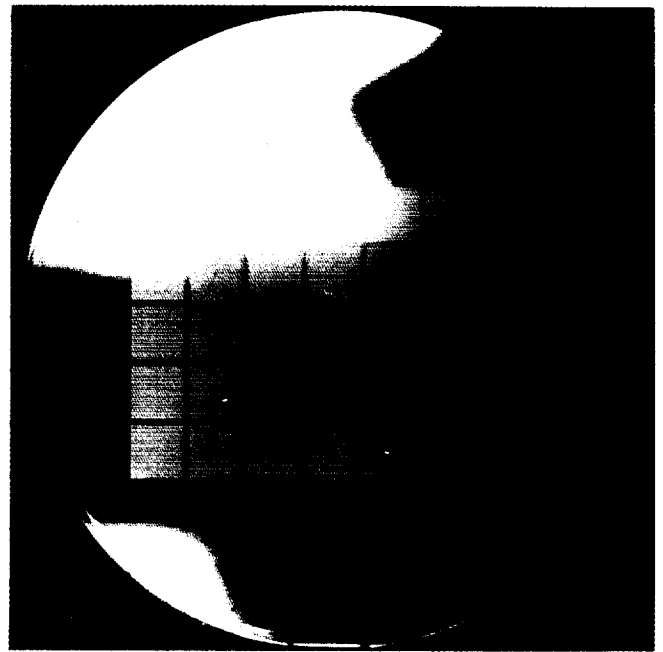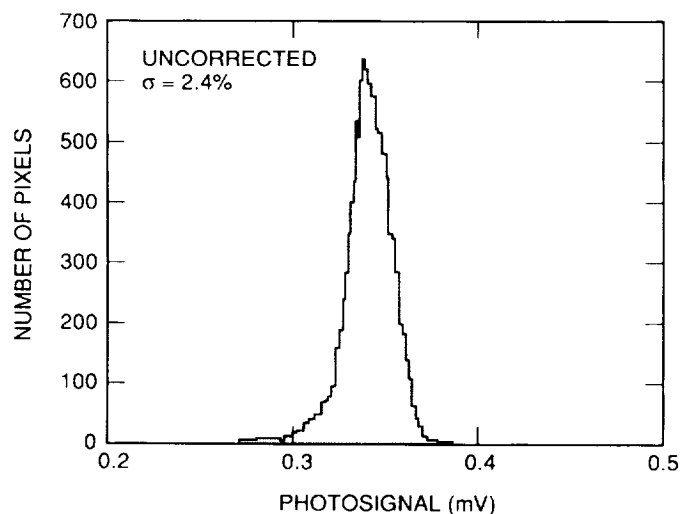
trapping efficiency of the random reflector is independent of the wavelength [12], as a consequence it preserves the spectral purity.

IV. IMAGING ARRAYS

The photoconductive QWIP's of the 128 × 128 FPA's were then fabricated by wet chemical etching through the photosensitive $GaAs/Al_xGa_{1-x}As$ multiquantum well layers into the 0.5-μm thick doped GaAs contact layer. Fig. 8 shows 35 128 × 128 QWIP focal plane arrays on a 3-in GaAs wafer. The pitch of the FPA is 50 μm and the actual pixel size is 38 × 38 μm^2. Then the random reflectors on the top of the detectors were covered with Au/Ge and Au for Ohmic contact and reflection. Then indium bumps were evaporated on top of the detectors for Si read out circuit (ROC) hybridization. A single QWIP FPA was chosen (cutoff wavelength of

Fig. 10.   One frame from a 15-μm QWIP video image of a man's face with $NE\Delta T = 30$ mK.

this sample is 14.9 μm) and bonded to a 128 × 128 Si multiplexer (Amber AE-159) and biased at $V_b = -2.7$ V. The FPA was back-illuminated through the flat thinned substrate (thickness ≈ 25 μm). Substrate thinning from 630 μm to 25 μm has tremendously reduced the optical cross-talk between neighboring pixels. However, thinning of the GaAs substrate to a membrane level will completely eliminate the optical cross-talk between pixels. Furthermore, it will enhance the light trapping efficiency of the random reflector and completely eliminate the thermal mismatch between the silicon readout multiplexer and the GaAs based QWIP focal plane array. This initial array gave excellent images with 99.9% of the pixels working, demonstrating the high yield of GaAs technology. Fig. 9 clearly shows the excellent uncorrected photocurrent uniformity (pixel-to-pixel) of the 16 384 pixels of the 128 × 128 FPA with a standard deviation of only $\sigma = 2.4$ %. The residual nonuniformity after correction was 0.05% and it is comparable to other types of focal plane arrays. Measurements were made to evaluate the variation of residual nonuniformity after two point correction as a function of scene temperature. According to these experiments the residual nonuniformity is less than 0.1% from 10 to 40 °C. This is a further indication that correctability is independent of random reflector and pixel-to-pixel lithography variations. As mentioned earlier this high yield is due to the excellent GaAs growth uniformity and the mature GaAs processing technology.

Video images were taken at various frame rates varying from 50 to 200 Hz with $f/2.3$ KRS-5 optics at temperatures as high as $T = 45$ K, using a ROC capacitor having a charge capacity of 4×10^7 electrons. Fig. 10 shows an image of a man's face taken with a QWIP FPA camera. The diffraction limited spot size of this 15-μm imaging camera is about 84 μm (i.e., $2.44 \cdot \lambda \cdot f\#$). Therefore, the minimum spatial resolution is four pixels and most of the fuzziness in the picture is attributed to this diffraction limitation. The measured noise equivalent temperature difference $NE\Delta T$ of the FPA was 30 mK at an operating temperature of $T = 45$ K for 300 K background. This reasonably agrees with our calculated value of 10 mK.

We have used the following equation to calculate the $NE\Delta T$ of the FPA:

$$NE\Delta T = \frac{\sqrt{AB}}{D_B^*(dP_B/dT)\sin^2(\theta/2)} \qquad (1)$$

where D_B^* is the blackbody detectivity, dP_B/dT is the derivative of the integrated blackbody power with respect to temperature, and θ is the field of view angle [i.e., $\sin^2(\theta/2) = (4f^2 + 1) - 1$, where f is the f number of the optical system]. No bandpass filters were used and are unnecessary in QWIP camera systems because of the narrow spectral response of QWIP's. It should be noted that these initial unoptimized FPA results are far from optimum. The QWIP device structures was not optimized; the gratings were also not optimized for the maximum light coupling efficiency; no microlenses were used; no antireflection coatings were used; the substrate was not thinned enough (the hybrid was thinned to 25 μm, however, it was not sufficient to improve the light coupling efficiency to small pixel and in fact this explains the slightly higher measured $NE\Delta T$); and finally the multiplexer used was a photovoltaic InSb multiplexer which is certainly not optimized to supply the proper bias and impedance levels required by photoconductive QWIP's. Implementation of these improvements should significantly enhance the QWIP focal plane array operating temperatures (i.e., 77 K for 10 μm and 55 K for 15 μm).

ACKNOWLEDGMENT

REFERENCES

[1] M. T. Chahine, "Sensor requirements for earth and planetary observations," in Proc. Innovative Long Wavelength Infrared Detector Workshop, Pasadena, CA, Apr. 24–26 1990, pp. 3–31.

[2] D. Duston, "BMDO's IS&T faces new hi-tech priorities," BMD Monitor, pp. 180–183, May 19, 1995.

[3] C. G. Bethea, B. F. Levine, M. T. Asom, R. E. Leibenguth, J. W. Stayt, K. G. Glogovsky, R. A. Morgan, J. D. Blackwell, and W. J. Parrish, "Long wavelength infrared 128 × 128 Al$_x$Ga$_{1-x}$As/GaAs quantum well infrared camera and imaging system," IEEE Trans. Electron Devices, vol. 40, pp. 1957–1963, Nov. 1993.

[4] L. J. Kozlowski, G. M. Williams, G. J. Sullivan, C. W. Farley, R. J. Andersson, J. Chen, D. T. Cheung, W. E. Tennant, and R. E. DeWames, "LWIR 128 × 128 GaAs/AlGaAs multiple quantum well hybrid focal plane array," IEEE Trans. Electron Devices, vol. 38, pp. 1124–1130, 1991.

[5] W. A. Beck, T. S. Faska, J. W. Little, J. Albritton, and M. Sensiper, presented at Proc. 2nd Int. Symp. 2–20-μm Wavelength Infrared Detectors and Arrays: Physics and Applications, Miami Beach, FL, Oct. 10–12, 1994.

[6] B. F. Levine, C. G. Bethea, G. Hasnain, V. O. Shen, E. Pelve, R. R. Abbott, and S. J. Hsieh, "High sensitivity, low dark current 10-μm GaAs quantum well infrared photodetectors," Appl. Phys. Lett., vol. 56, pp. 851–853, 1990.

[7] B. F. Levine, "Quantum well infrared photodetectors," J. Appl. Phys., vol. 74, pp. R1–R81, 1993.

[8] S. D. Gunapala, G. Sarusi, J. S. Park, T. L. Lin, and B. F. Levine, "Infrared detectors reach new lengths," Phys. World, pp. 35–40, Dec. 1994.

[9] S. D. Gunapala, J. S. Park, G. Sarusi, T. L. Lin, J. K. Liu, P. D. Maker, R. E. Muller, C. A. Shott, T. Hoelter, and B. F. Levine, "128 × 128 GaAs/Al$_x$Ga$_{1-x}$As quantum well infrared photodetector focal plane array for imaging at 15 μm," submitted for publication.

[10] H. C. Liu, Z. R. Wasilewski, and M. Buchanan, "Segregation of Si doping in GaAs-AlGaAs quantum wells and the cause of the asymmetry in the current–voltage characteristics of intersubband infrared detectors," *Appl. Phys. Lett.* vol. 63, pp. 761–763, 1993.

[11] W. A. Beck, "Photoconductive gain and generation-recombination noise in multiple-quantum-well infrared detectors," *Appl. Phys. Lett.*, vol. 63, pp. 3589–3591, 1993.

[12] G. Sarusi, B. F. Levine, S. J. Pearton, K. M. S. V. Bandara, and R. E. Leibenguth, "Improved performance of quantum well infrared photodetectors using random scattering optical coupling," *Appl. Phys. Lett.*, vol. 64, pp. 960–962, 1994.

Sarath D. Gunapala received the B.S. degree in physics from the University of Colombo, Sri Lanka, in 1980, and the Ph.D. degree in physics from the University of Pittsburgh, Pittsburgh, PA, in 1986. He studied properties of thin films as a Research Associate at Rutgers University, New Brunswick, NJ, from 1986 to 1988.

From 1988 to 1991, he was a Post Doctoral member of the technical staff at AT&T Bell Laboratories where he participated in the development of quantum well infrared photodetectors for infrared imaging. He joined the Jet Propulsion Laboratory, California Institute of Technology, Pasadena, in 1992, where he currently leads the quantum well infrared photodetector (QWIP) research group.
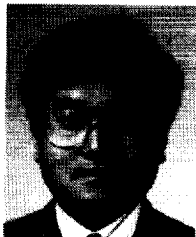
Jin S. Park received the B.S., M.S., and Ph.D. degrees in electrical engineering from the University of California, Los Angeles, in 1986, 1989, and 1992, respectively. His dissertation work involved Si/Ge molecular beam epitaxy and study of optical and transport properties of SiGe/Si quantum well/superlattice structures and their application in potential optoelectronic devices.

In 1992, he joined the Jet Propulsion Laboratory, California Institute of Technology, Pasadena, as a member of the technical staff, and conducted research/development of IR detectors and focal plane arrays utilizing III-V quantum wells and SiGe/Si heterostructures. In 1995, he joined the Intel Corporation, Santa Clara, CA. His current work involves development of 0.25-μm CMOS technologies.

Gabby Sarusi, photograph and biography not available at the time of publication.

True-Lon Lin, photograph and biography not available at the time of publication.

John K. Liu received the B.S. degree in engineering science (bioengineering) from the University of California, San Diego, in 1984, and the M.S.E.E. degree from the University of California, Los Angeles, in 1986.

From 1985 to 1989, he was with the Jet Propulsion Laboratory, California Institute of Technology, Pasadena, where he worked on solar cell and III–V MBE growth. From 1989 to 1991, he was with TRW, where he worked on III–V thin-film growth using MBE for MMIC applications. Since 1991, he has been with the Jet Propulsion Laboratory, working on the development of the QWIP IR camera. His current interest is QWIP FPA fabrications and characterizations.

Paul D. Maker received the Ph.D. degree in physics from the University of Michigan, Ann Arbor, in 1961.

He has worked in the fields of infrared molecular spectroscopy, lasers and nonlinear optics, hyper-Raman scattering, atmospheric chemistry, and automotive emissions analysis studied by long-path FTIR, and most recently, electron beam lithography and diffractive optics. Following a long career at the Ford Motor Company Scientific Research Laboratory, he joined the Jet Propulsion Laboratory, California Institute of Technology, Pasadena, in 1987, where he currently manages the electron beam lithography lab as a Technical Group Leader. His current research centers upon innovative uses of the electron beam machine, especially the fabrication of computer generated, e-beam fabricated holograms, and other diffractive optic devices.

Richard E. Muller received the B.S. degree in chemical engineering from the University of Rochester, Rochester, NY, in 1984.

He has worked in photolithography development at Commodore International and Microwave Semiconductor Corporation. He joined the Jet Propulsion Laboratory, Center for Space Microelectronics Technology, Pasadena, CA, in 1988. He is responsible for the operation of the JEOL JBX 5DII electron-beam lithography system, as well as the related sample processing.

Craig A. Shott received the B.S. degree from the University of California, Santa Cruz, in 1985. He pursued graduate-level coursework in solid state electrical engineering at the University of California, Santa Barbara, while working at Santa Barbara Research Center.

Since 1989, he has been with the Amber Engineering, a Raytheon Company, Goleta, CA, were he is currently Manager of Advanced Processes, and has developed processes for HgCdTe, InSb, GaAs QWIP, and SiGa FPA devices. His most recent work involves developing processes for uncooled Microbolometer device fabrication.
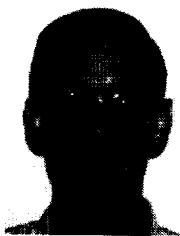
Ted Hoelter received the B.S. degree in physics from the University of California, Santa Barbara.

Currently, he is a Product Engineer in the Standard Products Group, Amber Engineering, A Raytheon Company, Goleta, CA, where he is primarily responsible for matching special customer needs with Amber's standard line of IR imaging products and, when necessary, modifying standard products for custom applications.